

THE USE OF BURMESTER CURVES IN COMBINATION WITH THE LEAST SQUARE METHOD IN THE DESIGN OF THE STEPHENSON-I TYPE MECHANISM

B. Pira and L. Topilla*

Faculty of Engineering and Informatics, University of Applied Sciences in Ferizaj, KOSOVO
E-mail: labinot.topilla@ushaf.net

This paper provides a brief description of an approach that utilises Burmester curves in designing six-bar mechanisms that prescribe five precision points. This approach combines the Freudenstein method and the least square method with Burmester theory. With this paper, we demonstrate the application of this combined approach in designing Stephenson type-I six-bar planar mechanisms that prescribe five positions, using a specific case study. The results show that there is a means of combining the three methods in the design of the six-bar mechanism of Stephenson I type and generating the fixed and moving points of the six-bar where the structural error (the difference between the desired output angle and the generated angle) is minimised.

Key words: Burmester, mechanism, design, least square, six-bar.

1. Introduction

Nowadays, are often encounter various types of mechanisms without always recognising their presence [1]. Mechanisms are present in diverse forms: two-dimensional, three-dimensional, involving sliding, rolling, or combined movements. Their primary function is to execute specific tasks, such as relocating objects between different positions or defining, or rather prescribing, a particular path and or performing a certain function or motion [2]. Though four-bar mechanisms, with one degree of freedom, can perform many tasks, six-bar mechanisms can introduce more complex functions to the mechanisms [3].

One of the most important motion characteristics of a mechanism is achieved accurately only at certain specific points, while structural errors remain present at all other positions. Utilising the least squares method, structural errors are optimised and compared with previous findings. Choi *et al.* introduced stochastic linkage models for analysing mechanical errors in planar mechanisms [4]. These models account for tolerances and clearances to analyse the effects on planar mechanisms, with the subsequent discussion of the results. At the same time, adjustable mechanisms offer versatile outputs suitable for various industries. Zhou introduced an optimal synthesis approach to determine the most efficient adjustment [5]. By continuously adjusting or fixing adjustment joints, precise or approximate desired functions can be generated accordingly. The combination of Burmester curves and least square method [6], will be shown using an extreme case where a mechanism has to prescribe five precision positions.

Though there have been attempts to utilise the Burmester theory in the syntheses of Stephenson types of six-bar mechanisms using coordinate parameterisation for the ternary link [7], in this paper the Burmester theory is utilised in combination with the Inversion Method in the design of a Stephenson-I type of six-bar mechanism that will prescribe five precision points as well as keep the desired angle of the element moved by the mechanism. On the other hand, various authors looked at the optimisation of the motion generation by way of reducing the structural error.

* To whom correspondence should be addressed

2. Theoretical applications

There are two and three infinite possibilities for designing a mechanism when a body moves through two and three prescribed positions, respectively. On the other hand, there is only one infinite and a few conceivable designs for mechanisms when the body moves through four or five prescribed positions. By employing complex numbers, Burmester was able to solve the difficulty of the plane's four specified positions [6] (Fig.1).

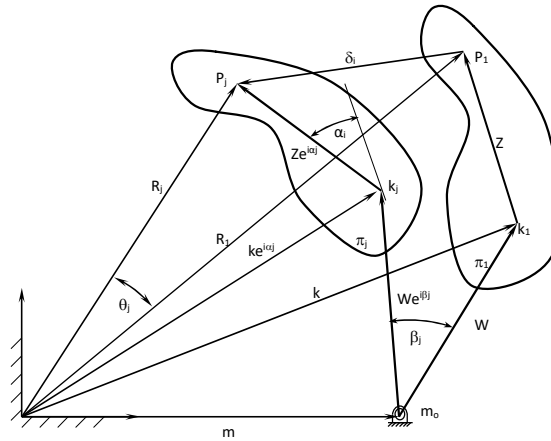


Fig.1. The unknown dyad's W, Z which can guide the moving plane π from the first to the j -th position [8].

One can notice that the vectors defined above form a closed loop, including the first and j -th positions [8]:

$$\vec{W}e^{i\beta_j} + \vec{Z}e^{i\alpha_j} - \vec{\delta}_j - \vec{Z} - \vec{W} = 0. \tag{1.1}$$

After the compatible sets of β_2 are obtained, any method for solving simultaneous complex equations can be used to find Z and W . Then the circle point k and the centre point m are given by the following expressions (Fig.1).

$$k = R_j - Z \quad \text{and} \quad m = k - W. \tag{1.2}$$

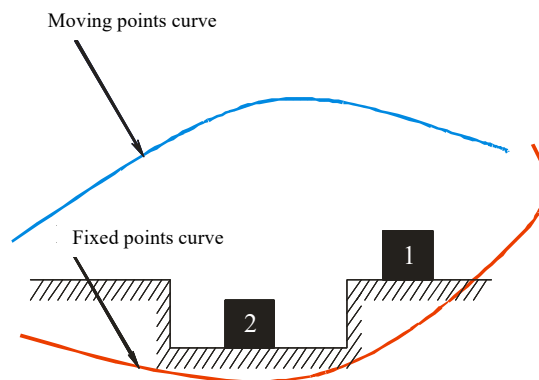


Fig.2. Visualisation of the Burmester curves application [14].

The above pair of these two points is called the Burmester point pair (B.P.P.), and the locus of these pairs for different values of β_2 form the Burmester curves. Practically, the Burmester method generates two types of curves:

- Fixed point curve and
- Circle (moving) point curve.

Fixed or ground points are the points (links/joints) in which the mechanism is connected to the ground, while the circle points are the points (links/joints) of movement of the mechanism. From these points, the mechanism is constructed which enables the repositioning of the object (Fig.2) from position 1 to position 2.

2.1. Application of Burmester theory in Stephenson-I Type of mechanisms

Chan utilised Burmester theory with a specially written computer program [1]. It calculated circle (moving) point and fixed (centre) point curves (specific for Burmester theory) for four positions. However, for more than four precision points, the application of the Burmester curves can be achieved is the five precision points are split into two groups of four precision position, for example, the initial five precision points (1, 2, 3, 4, 5) were split into two groups of four precision points (1, 2, 3, 4 and 1, 2, 3, 5).

Noussas in 1996 [9] modified the computer program which generated two sets of Burmester curves for two groups of precision points. This program was later modified by the co-author of this paper, Pira and made it into a user-friendly application [10].

The two sets of Burmester curves generated by the program were superimposed on one another and at the points of intersection of fixed pint curves are generated the fixed (ground) points of the mechanism. The same goes for the circle (moving) point of the mechanism, which can be located at the points of intersection of circle point curves.

2.2. Six bar mechanisms

There are various types of six-bar mechanisms; however, the Stephenson and Watt six-bar mechanisms stand out as the only ones where all the joints of the bars (kinematic pairs) involve rolling connections without any sliding kinematic pairs. As shown in the Fig.3, three types of Stephenson six-bar mechanisms and two types of Watt six-bar mechanisms [11].

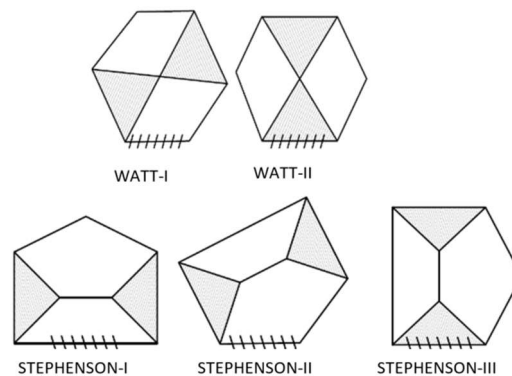


Fig.3. Watt and Stephenson six-bar mechanisms.

2.1. Synthesis of six-bar mechanisms

Constructive requirements may require the performance of a specific movement using a six-bar mechanism of Stephenson type-I. This special type of six-bar mechanism, just like the six-bar mechanism of Stephenson type-III and Watt-II, is made of the basic four-bar mechanism, while the difference between them is the remaining dyad, which in Stephenson type of mechanism has a special connection with the four-bar

(Fig.4). This means that it is very difficult or impossible to find a solution to a problem of a six-bar mechanism Stephenson type-I [12]. One possible solution was to form a Stephenson type-I path generator using the Stephenson type-III function generator [13].

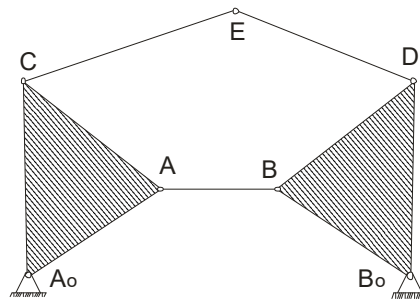


Fig.4. Stephenson-I type of six-bar mechanism.

There are two ways in which the Stephenson-I type of six-bar mechanism is designed with the combination of Burmester Curves and:

- inversion method and
- least square method

The combination of the Burmester curves and the Inversion method was already proven to be operational by inverting the six-bar mechanism in two four-bar mechanisms, identifying fixed as well as circle points of the four-bar finally integrating the mechanism [14].

The Burmester curves in combination with the least squares method generate the six-bar mechanism, prescribing precision points by separating the Stephenson-I mechanism into three sets of four-bar mechanisms (Fig.5). The two four-bar mechanisms (Ao-C-E-O and O-E-D-Bo) have a virtual link (O-E) while the remaining four-bar mechanism (Ao-A-B-Bo) is the main four-bar.

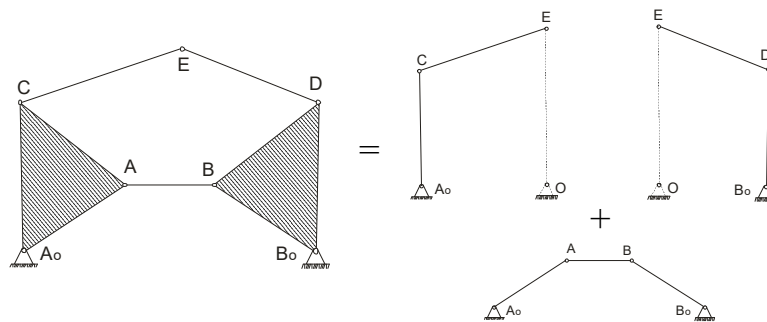


Fig.5. Separation of Stephenson-I into three sets of four-bar mechanisms.

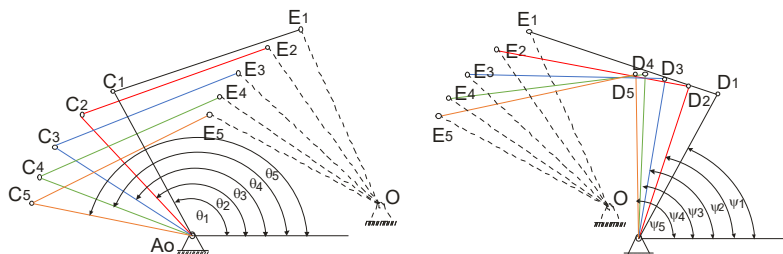


Fig.6. Two of the transformed STEHPENSON-I six-bar mechanism into two four-bar mechanisms with a virtual link.

As shown in Fig.6, the four-bar mechanisms consist of two main dyads (shown in full lines) as well as a virtual link, which can be the crank (leading) for one four-bar and at the same time as a follower to the other four-bar mechanism. The common element of both four-bar mechanisms are precision points which must be prescribed by both mechanisms.

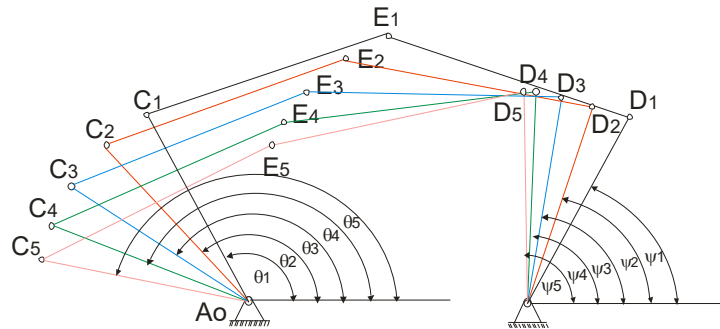


Fig.7. Newly joined Stephenson-I six-bar mechanism which prescribes five precision points.

Figures 6-7 show that the link Ao-C, as part of a dyad Ao-C-E, for the point E to prescribe all required positions, should be rotated to a certain angle θ_i , where $i = 1 \div 5$ from the horizontal line. θ_1 minimum angle is also an initial corner of link Ao-C, while the angle which the link prescribes is equal to:

$$\Delta\theta = \theta_5 - \theta_1. \tag{1.3}$$

The same applies to other four-bar mechanism, Bo-D respectively, as part of dyad Bo-D-E. After the execution of the Burmester's curves program, the curves obtained will generate two virtual four-bar mechanisms and with animation and analysis of this mechanism, its crank and followers angles θ_i and ψ_i , where $i = 1 \div 5$, will be known.

The main four-bar (Fig.5) crank and follower links are rigidly connected to Ao-C levels, respectively Bo-D, of the main part (main four-bar) of the six-bar mechanism. Therefore, the corresponding crank and followers angles, θ_i and ψ_i , where $i = 1 \div 5$, are the respective angles of the crank and followers of the main four-bar (Ao-A-B-Bo) as shown in Fig.8.

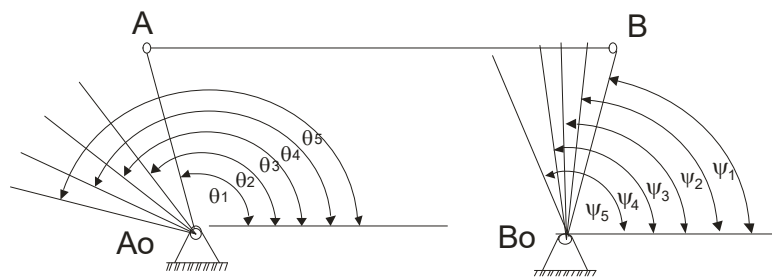


Fig.8. Main four-bar of the Stephenson-I six-bar mechanism.

2.2. Gauss method of least squares

When the angles through which both links will pass, crank as well as the follower, are defined and with the known fixed points of the mechanisms, i.e. the distance between these two points, then we can apply Freudenstein's equation, combining it with the Gauss method of least squares.

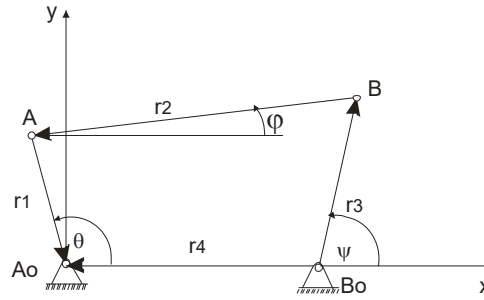


Fig.9. Analysis of main four-bar of the Stephenson-I six-bar mechanism.

Freudenstein in 1954 introduced the analytical technique of mechanism synthesis. This algebraic method uses the equation Freudenstein to shift the four-bar mechanism for prescribing of three precision points [15]. From Fig.9, it can be seen that the links in the four-bar form a closed loop vector which can be represented with the equation:

$$\vec{r}_1 + \vec{r}_2 + \vec{r}_3 + \vec{r}_4 = 0. \tag{1.4}$$

By projecting this equation in both x and y axes we have two equations:

$$r_1 \cdot \cos \theta + r_2 \cdot \cos \theta + r_3 \cdot \cos \psi - r_4 = 0, \tag{1.5}$$

$$r_1 \cdot \sin \theta + r_2 \cdot \sin \theta + r_3 \cdot \sin \psi - r_4 = 0. \tag{1.6}$$

Once both sides of the equations are squared and then by adding both of the equations we have:

$$r_2^2 = r_1^2 \cdot r_3^2 \cdot r_4^2 - 2 \cdot r_4 \cdot r_1 \cdot \cos \theta + r_3 \cdot r_4 \cdot \cos \psi - 2 \cdot r_1 \cdot r_3 \cdot (\cos \theta \cdot \cos \psi + \sin \theta \cdot \sin \psi). \tag{1.7}$$

By substituting $(\cos \theta \cdot \cos \psi + \sin \theta \cdot \sin \psi) = \cos(\theta - \psi)$ we'll have:

$$\frac{r_4^2 + r_3^2 + r_1^2 - r_3^2}{2 \cdot r_1 \cdot r_3} + \frac{r_4}{r_3} \cdot \cos \theta - \frac{r_4}{r_1} \cdot \cos \psi = -\cos(\theta - \psi) \tag{1.8}$$

or in a simpler form:

$$R_1 + R_2 \cdot \cos \psi - R_3 \cdot \cos \theta - \cos(\theta - \psi) = 0 \tag{1.9}$$

where:

$$R_1 = \frac{r_4^2 + r_3^2 + r_1^2 - r_3^2}{2 \cdot r_1 \cdot r_3}, \quad R_2 = \frac{r_4}{r_1}, \quad R_3 = \frac{r_4}{r_3},$$

r_1, r_2, r_3 and r_4 – links of the four-bar mechanism,

θ_i – angle between x axis and the crank,

ψ_i – angle between y axis and the follower.

In the general form Eq.(1.7) will look like this:

$$R_1 + R_2 \cdot \cos \psi_j - R_3 \cdot \cos \theta_j - \cos(\theta_j - \psi_j) = 0 \quad (1.10)$$

where: j - number of precision points

The last equation is also known as Freudenstein's equation. The flaw in this equation is that generates solutions for mechanisms which prescribe just three precision points. For more than three precision points, Freudenstein's equation can be expanded by taking into account the structural error or mistakes of the mechanism [16]. In reality, it is almost impossible to implement the ideal movement of the mechanism through its precision points. This means that there is a structural error e_j which appears in this way:

$$e_j = R_1 + R_2 \cdot \cos \psi_j - R_3 \cdot \cos \theta_j - \cos(\theta_j - \psi_j). \quad (1.11)$$

Squares of the error e_j for n positions are calculated this way:

$$F = \sum_{j=1}^n e_j^2 = \frac{1}{n-1} \cdot \sum_{j=1}^n \left[R_1 + R_2 \cdot \cos \psi_j - R_3 \cdot \cos \theta_j - \cos(\theta_j - \psi_j) \right]^2. \quad (1.12)$$

Again, if we want to have a least errors as possible:

$$\frac{\partial F}{\partial R_1} = \frac{\partial F}{\partial R_2} = \frac{\partial F}{\partial R_3} = 0. \quad (1.13)$$

Equation $1/(n-1)$ will be neglected for being 1 for a large number of positions, and with the execution of the partial differentiation of F , we have:

$$\begin{aligned} \frac{\partial F}{\partial R_1} &= \sum_{j=1}^n \left[R_1 + R_2 \cdot \cos \psi_j - R_3 \cdot \cos \theta_j - \cos(\theta_j - \psi_j) \right] = 0, \\ \frac{\partial F}{\partial R_2} &= \sum_{j=1}^n \left[R_1 + R_2 \cdot \cos \psi_j - R_3 \cdot \cos \theta_j - \cos(\theta_j - \psi_j) \right] = 0, \\ \frac{\partial F}{\partial R_3} &= \sum_{j=1}^n \left[R_1 + R_2 \cdot \cos \psi_j - R_3 \cdot \cos \theta_j - \cos(\theta_j - \psi_j) \right] = 0. \end{aligned} \quad (1.14)$$

After partial differentiation, we get:

$$\begin{aligned} R_1 + R_2 \sum_{j=1}^n \cos \psi_j - R_3 \sum_{j=1}^n \cos \theta_j - \sum_{j=1}^n \cos(\theta_j - \psi_j) &= 0, \\ R_1 \sum_{j=1}^n \cos \psi_j + R_2 \sum_{j=1}^n \cos^2 \psi_j - R_3 \sum_{j=1}^n \cos \theta_j \sum_{j=1}^n \cos \psi_j - \sum_{j=1}^n \cos(\theta_j - \psi_j) \sum_{j=1}^n \cos \psi_j &= 0, \end{aligned} \quad (1.15)$$

$$\begin{aligned}
 &R_1 \sum_{j=1}^n \cos \theta_j + R_2 \sum_{j=1}^n \cos \psi_j \sum_{j=1}^n \cos \theta_j - R_3 \sum_{j=1}^n \cos^2 \theta_j - \\
 &+ \sum_{j=1}^n \cos(\theta_j - \psi_j) \sum_{j=1}^n \cos \theta_j = 0.
 \end{aligned}
 \tag{1.15} \text{ cont.}$$

These equations are applied to each set of precise points. The chosen values are simply summarized under the summation sign, from which R_1, R_2 and R_3 are calculated. Given there are four links, r_1, r_2, r_3 , and r_4 , in a four-bar mechanism, and only three equations, one side needs to be chosen. It's recommended to choose r_4 .

Given that during the mechanism's operation, structural errors or losses actually exist, the aim is to minimize them. Structural error is calculated in the following way.

$$\varepsilon_s = \frac{\Psi_g - \Psi_d}{\Psi_g} 100[\%].
 \tag{1.16}$$

This error, in other words, represents nothing more than the difference between the desired angle and the calculated one. In (Fig.10), the scheme of the difference between the desired and calculated angles is presented in a general form.

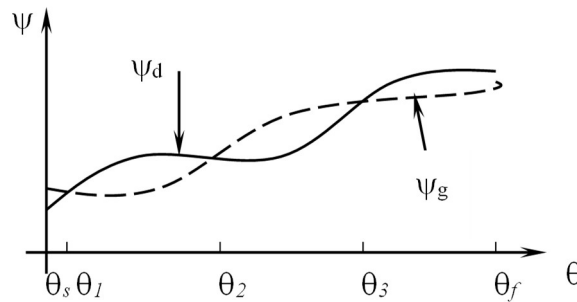


Fig.10. Structural error.

An application of the fundamental square Gauss method is presented in the case study.

3. Examples of application

It is considered a specific case where it is required to design a six-bar mechanism of the Stephenson-I type, which should accurately describe 5 points (Tab.1).

Table 1. The coordinates of the points that the mechanism needs to describe, for both bars.

Positions	Coordinates of the positions		Crank angle θ°	Follower's angle ψ°
	X	Y		
1	0.000	0.000	0	0
2	-0.625	-0.202	-10	10
3	-1.00	-0.625	-20	20
4	-1.250	-1.250	-30	35

After dividing the six-bar mechanism into two four-bar mechanisms, data input into the 'BurCurves' program begins for both four-bar mechanisms, and two pairs of Burmester loops will be obtained. The first loop concerns the representation of possibilities for finding the main points (nodes) of both pairs of four-bar mechanisms. Figure 11 illustrates the first loops representing the movement of one link of the six-bar mechanism.

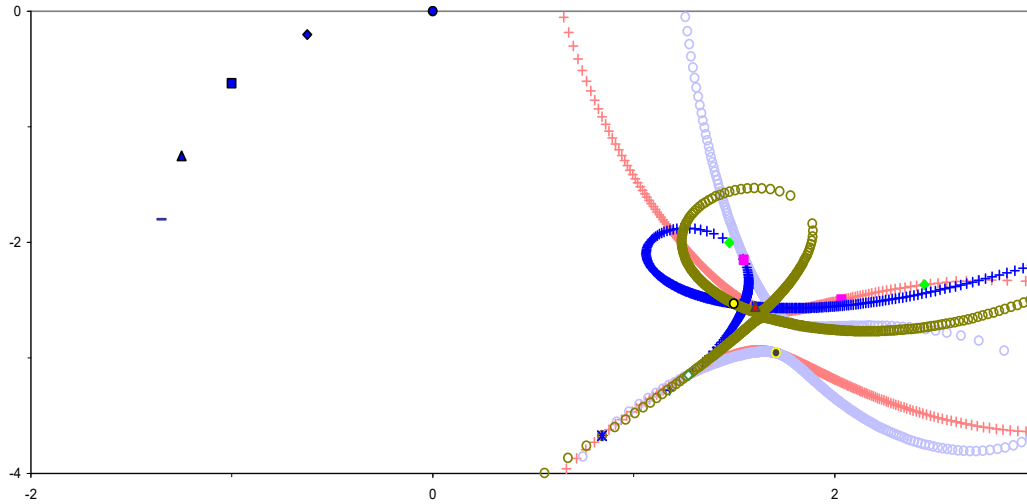


Fig.11. Burmester curves for one of the four-bars.

The same applies to the other four-bar mechanism as shown in Fig.12, in which case the superimposition of that part of the mechanism is implemented according to the specific requirements of the problem.

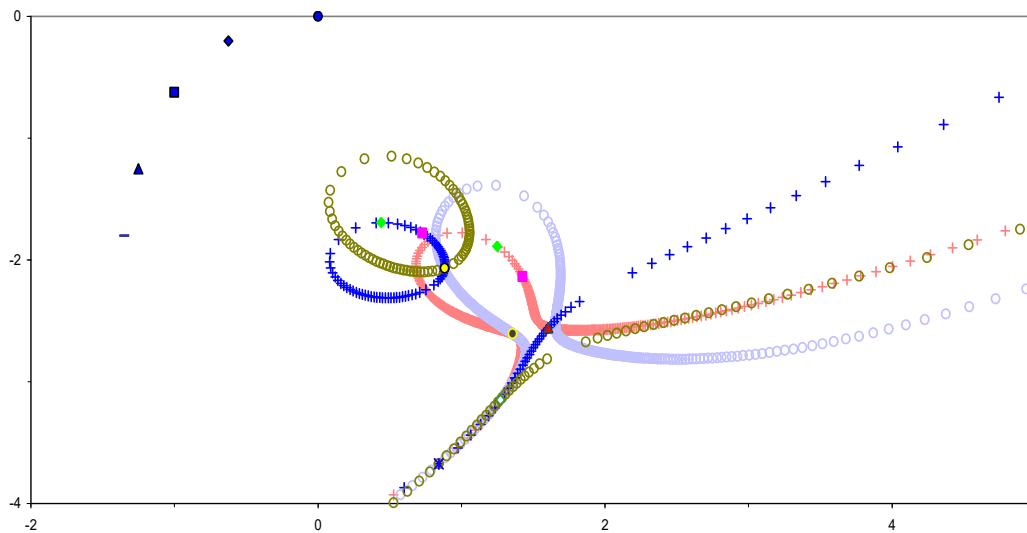


Fig.12. Burmester curves for the remaining four-bar.

From both sets of curves, certain number of possible fixed and circle points of the Stephenson-I six-bar mechanism are obtained. Table 2 presents the coordinates of the possible circle and fixed points of the mechanism.

Table 2. The coordinates of the possible fixed and circle points of the six-bar mechanism.

Nr	First pair of curves		Second pair of curves	
	Fixed points	Circle points	Fixed points	Circle points
1	1.17; -1.90	1.44; 1.59	0.75; -2.25	0.98; -1.49
2	1.61; -2.56	1.68; -2.55	0.81; -1.86	0.87; -2.06
3	1.55; -2.51	1.79; -2.71	1.61; -2.56	1.77; -2.64
4	1.86; -2.57	1.87; -2.73	2.69; -2.43	2.41; -2.74

Figures 13-14 illustrate the main parts of the six-bar mechanism superimposed on Burmester curves.

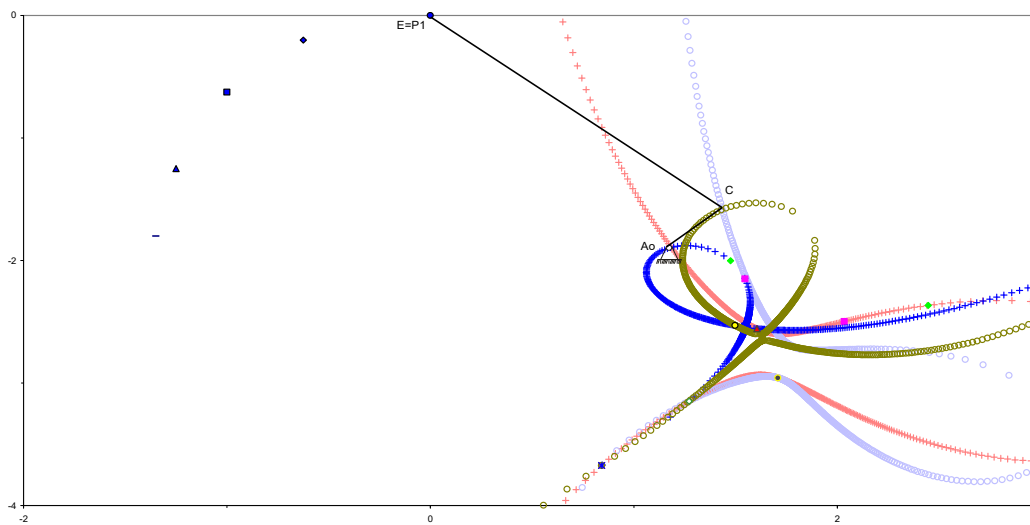


Fig. 13. Part of the mechanism presented (superimposed) on the Burmester curves in the first position.

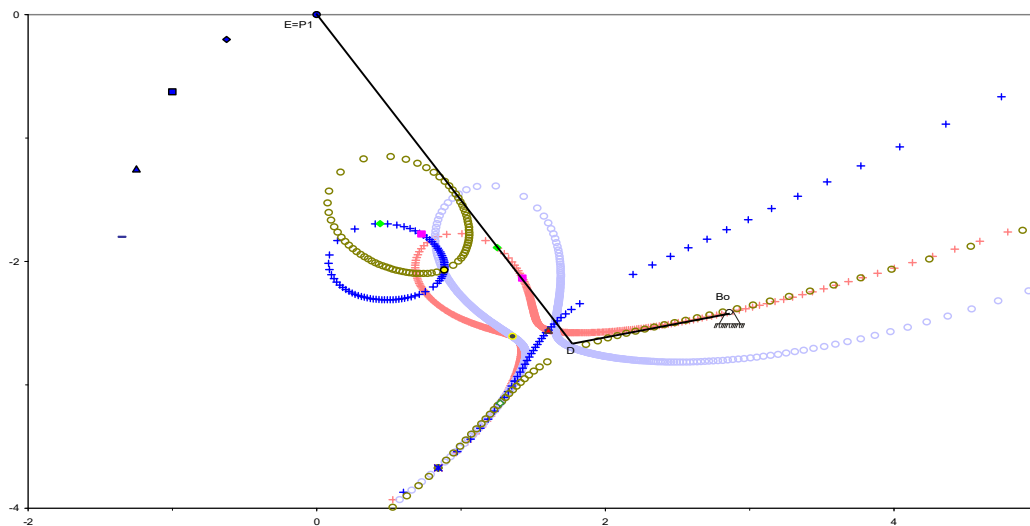


Fig. 14. Part of the mechanism presented (superimposed) on the Burmester curves for the second dyad.

These points are generated from the intersection of centre curves. The same applies to circular curves as well. And by making possible combinations of coordinates of fixed and, respectively, circle points and animating them using the DeMEC program, the most suitable combination of points has been found and presented in Tab.3, which indeed forms the Stephenson-I six-bar mechanism in its initial position.

Table 3. Coordinates of fixed and circle points of the base six-bar mechanism in the initial position (excluding the main four-bar).

Coordinates of the positions	Fixed (ground) points		Circle (moving) points	
	Ao	Bo	C	D
<i>X</i>	1.17	2.69	1.44	1.77
<i>Y</i>	-1.90	-2.43	1.59	-2.64

By combining these two diagrams of the mechanism, the main part of the Stephenson-I six-bar mechanism was obtained, describing all the required positions (Fig.15).

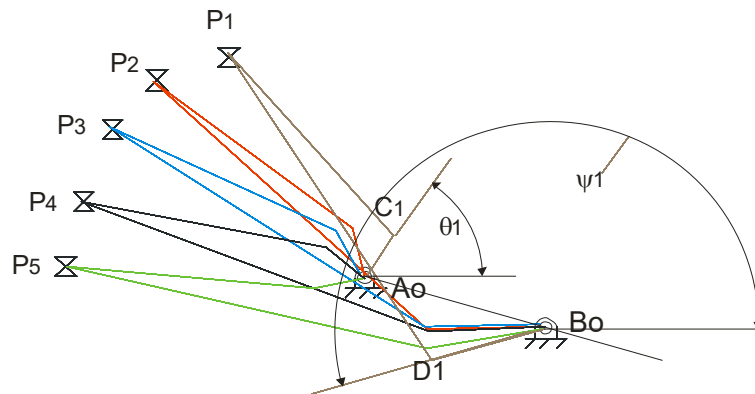


Fig.15. The combined diagrams passing through the five required points.

Analysing the angles that will close both dyads' angles of the six-bar mechanism (Fig.13), the changes in the angles Δθ and Δψ, angles were obtained and are presented in the Tab.4.

Table 4. The value of the angles that close both dyads angles with the *x*-axis.

Positions	Angle of the	
	first dyad Δθ	second dyad Δψ
1	0	0
2	42.592	-14.518
3	71.177	-18.627
4	105.123	-18.066
5	153.361	-2.023

Knowing the angles that need to describe both the crank and the follower, and also knowing the distance between two fixed points of the six-bar mechanism (which are also the fixed points of the four-bar mechanism), namely link *r*₄, the Gauss square method (GSM) can be applied. For easier application of GSM, a table has been designed in Microsoft Excel through which, using the trial and error method, considering the minimization of structural error, the optimal solution of the four-bar mechanism is achieved.

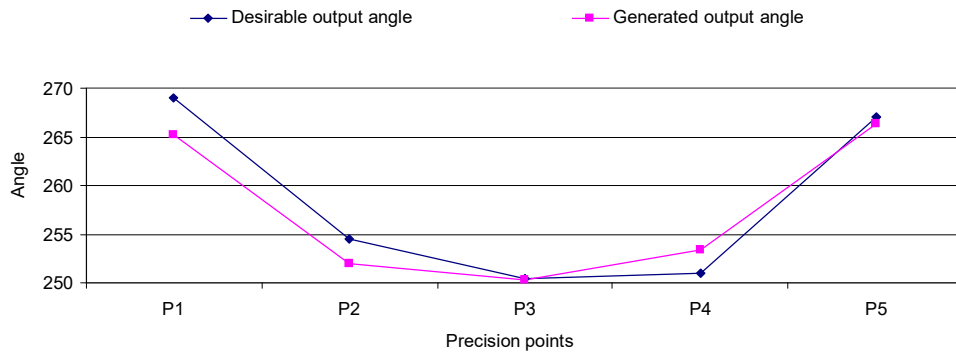


Fig.16. The difference between the desired input angle and the generated input angle.

Ultimately, for the initial input angle of 203° and the output angle of 269° , the most suitable part of the four-bar mechanism of the six-bar type Stephenson-I has been identified, where the structural error, meaning the difference between the desired output angle and the generated one, is minimized. Figure 16 illustrates the graph of the structural error, specifically the difference between the output (working) angles.

In conclusion, by integrating the two structures of the six-bar mechanism, the Stephenson-I mechanism was obtained, as presented in Fig.17 and in its initial position.

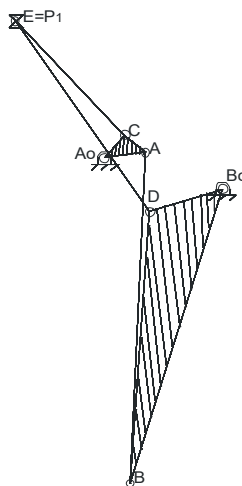


Fig.17. The six-bar mechanism of the Stephenson-I type in the initial position.

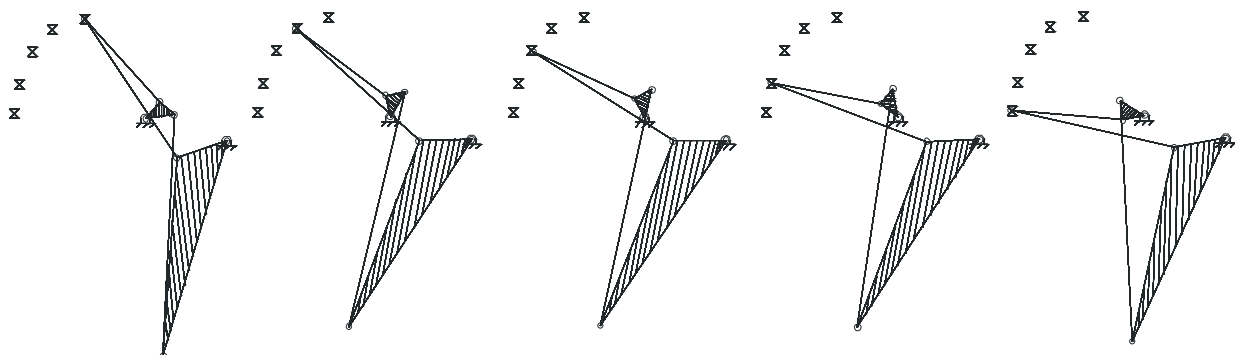


Fig.18. The Stephenson-I type six-bar mechanism prescribing five specified positions.

Using the motion simulation program, the Stephenson-I type six-bar mechanism is animated and illustrated in Fig.18. The mechanism clearly demonstrates how it passes through the five precision points and performs the cutting procedures.

4. Conclusions

This work takes a step further into Burmester's theory and its application in the synthesis of six-bar mechanisms of Watt-II and Stephenson-I and III types. It's worth mentioning that these mechanisms have a specific structure that complicates its synthesis. In all studied cases, in order to address their synthesis, six-bar mechanisms are divided into two groups of four-bar mechanisms.

Furthermore, this work demonstrates that Burmester's theory can be integrated with simple graphic and analytical methods of mechanism synthesis, such as the inverse method, Freudenstein's method (or the least square method), etc. Successful results in the synthesis of six-bar mechanisms have been achieved through the combination of Burmester's method with the inverse method. The simplicity of the inverse method has been employed in all studied cases, but its drawback is that it is a graphical method that may result in measurement errors, although those errors are very small. On the other hand, the application of the least square method solves the problem of measurement errors. Also, the application of the least square method can be utilised in optimising the solution of the most suitable mechanism by reducing structural errors.

The Stephenson-I type mechanism has an even more complicated structure than the Watt-II type. In this work, two ways of designing this mechanism have been demonstrated. The method that has provided better results and greater accuracy (smaller error in the structure of the mechanism) is the integration of Burmester's theory with the Gauss least square method.

Everything done in this work leads us to appear that Burmester's theory, with some modifications, opens the possibility of its application in designing six-bar mechanisms of other types. The author's recommendations are to expand Burmester's theory to cover even broader aspects of designing not only six-bar mechanisms but also other multi-link structures/mechanisms, incorporating various kinematic groups.

Nomenclature

- A_0, B_0 – fixed (ground) points of the mechanism
- C, D – circle (moving) points of the mechanism
- e_j – structural error
- F – squares of the error
- i – number of prescribed precision points
- j – number of precision points
- P_i – prescribed precision points
- r – links of the mechanism
- X, Y – coordinates of the positions
- ε_s – angle structural error in percentage
- $\Delta\theta$ – delta (changes) in the rotating angle of the crank
- $\Delta\psi$ – delta (changes) in the rotating angle of the follower
- θ – the rotating angle of the crank
- ψ – the rotating angle of the follower
- ψ_d – desired angle
- ψ_g – calculated angle

References

- [1] Chan Y. (1994): *Some Case Studies in Mechanism Design*.– MSc Thesis, London, Department of Mechanical Engineering, Imperial College.
- [2] Tsai L.-W. (2001): *Mechanism Design: Enumeration of Kinematic Structures According to Function*.– 1st ed., CRC Press.
- [3] Shen Q., Lee W.-T., Russell K. and Sodhi R.S. (2008): *On motion generation of Watt I mechanisms for mechanical finger design*.– Trans, CSME, vol.32, No.3-4, pp.411-421.
- [4] Choi J., Lee S. and Choi D. (1998): *Stochastic linkage modeling for mechanical error analysis of planar mechanisms*.– Mechanics of Structures and Machine, vol.26, No.3, pp.257-276. <https://doi.org/10.1080/08905459708945494>.
- [5] Zhou H. (2009): *Synthesis of adjustable function generation linkages using the optimal pivot adjustment*.– Mechanism and Machine Theory, vol.44, No.5, pp.983-990. <https://doi.org/10.1016/j.mechmachtheory.2008.05.016>.
- [6] Jha A.S. and Verma M. (2018): *Error reduction in data prediction using least square regression*.– International Research Journal of Engineering and Technology, vol.5, No.12, pp.703-706.
- [7] Bai S., Wang D. and Dong H. (2016): *A unified formulation for dimensional synthesis of Stephenson linkages*.– Journal of Mechanisms and Robotics, vol.8/041009-1, <https://doi.org/10.1115/1.4032701>.
- [8] Sandor G. and Erdman A. (1984): *Advanced Mechanism Design: Analysis and Synthesis*.– 2nd ed., Pearson.
- [9] Noussas D. (1996): *Case Studies in Mechanism Design*.– Msc thesis, London, Department of Mechanical Engineering, Imperial College.
- [10] Pira B. (1999): *The use of Burmester Curves in Design of Planar Mechanisms*.– London: Department of Mechanical Engineering, Imperial College.
- [11] Pira B., Bajraktari A., Cunaku I. and Ymeri M. (2011): *Synthesis of mechanisms with more than four bars using Burmester theory*.– Vienna, Annals of DAAAM for 2011 & Proceedings of the 22nd International DAAAM Symposium, vol.22, No.1, ISSN 1726-9679.
- [12] Hall A.S.J. (1961): *Kinematics and Linkage Design*.– 1st ed., Prentice Hall.
- [13] Plecnik M.M. (2015). *The Kinematic Design of Six-bar Linkages Using Polynomial Homotopy Continuation*.– UC Irvine, retrieved from <https://escholarship.org/uc/item/3sb8s541>.
- [14] Pira B., Buza K., Gojani I., Pajaziti A., Anxhaku A. (2006): *Design of Stephenson-I Type of six-bar mechanism using Burmester curves and inversion method*.– Barcelona, Trends in the Development of Machinery and Associated Technology.
- [15] Freudenstein F. (1954) *Design of Four-link Mechanisms*.– Ph. D. Thesis, Columbia University, USA.
- [16] Mehar K., Singh S. and Mehar R. (2015): *Optimal synthesis of four-bar mechanism for function generation with five accuracy points*.– Inverse Problems in Science and Engineering, vol.23, No.7, pp.1222-1236.

Received: December 22, 2024

Revised: June 14, 2025